energies

MDPI

Article

Battery Energy Storage Systems in Microgrids: Modeling and Design Criteria

Matteo Moncecchi [1,*], Claudio Brivio [2], Stefano Mandelli [3] and Marco Merlo [4]

1 Department of Energy, Politecnico di Milano, Via Lambruschini, 4, 20156 Milano, Italy
2 CSEM SA - Swiss Center for Electronics and Microtechnology, 2002 Neuchâtel, Switzerland; claudio.brivio@csem.ch
3 CESI S.p.A., Via Raffaele Rubattino, 54, 20134 Milano Italy; stefano.mandelli@cesi.it
4 Politecnico di Milano, Department of Energy, Via Lambruschini, 4, 20156 Milano, Italy; marco.merlo@polimi.it
* Correspondence: matteo.moncecchi@polimi.it; Tel.: +39-02-2399-3762

Received: 12 March 2020; Accepted: 8 April 2020; Published: 17 April 2020

Abstract: Off-grid power systems based on photovoltaic and battery energy storage systems are becoming a solution of great interest for rural electrification. The storage system is one of the most crucial components since inappropriate design can affect reliability and final costs. Therefore, it is necessary to adopt reliable models able to realistically reproduce the working condition of the application. In this paper, different models of lithium-ion battery are considered in the design process of a microgrid. Two modeling approaches (analytical and electrical) are developed based on experimental measurements. The derived models have been integrated in a methodology for the robust design of off-grid electric power systems which has been implemented in a MATLAB-based computational tool named Poli.NRG (POLItecnico di Milano—Network Robust desiGn). The procedure has been applied to a real-life case study to compare the different battery energy storage system models and to show how they impact on the microgrid design.

Keywords: energy storage; battery models; microgrids; rural electrification; developing countries; optimization

1. Introduction

Rural electrification represents one of the issues to be faced in order to provide energy services to 1.2 billion people living in Developing Countries (DCs) that do not have access to electricity [1]. Off-grid systems have an important role in this issue, and especially electrical power systems based on photovoltaic (PV) and battery energy storage systems (BESS). In the rest of this section a brief literature review of the methodologies and software that already address this issue is presented. Several gaps could be detected; this motivates the alternative design procedure discussed in this paper. Section 2 describes the features of the methodology for the robust design of off-grid electric power systems. Off-grid systems strongly rely on energy storage, consequently BESS models are investigated in Section 3. Finally, Section 4 introduces the study case in which the proposed methodology and BESS models are applied to a rural village of Tanzania. Results of the study case are presented in Section 5, where a detailed comparison of the different battery models evaluated aims at understanding their impact on the power system design.

The design process of off-grid systems is not straightforward since it means matching unpredictable energy sources with unknown or uncertain load demands and, at the end, providing the most favorable conditions in terms of reliability and costs. Within the scientific literature, there are three main methods to design off-grid power systems [2]. Each of them requires data about user's

load and energy resources. These input data may vary in terms of temporal detail and accuracy in measurement or estimation.

Actually, commercial software based on the above presented methodologies are already available. Sinha and Chandel [3], and Khatib et al [2] reviewed software tools to size off-grid power systems. HOMER by NREL [4] is the most used software for the simulation and optimization of off-grid hybrid power systems. It determines the configuration that minimizes life-cycle costs for a particular site application. RETScreen by CANMET [5] is a renewable energy decision support and capacity building tool. TRNSYS by Solar Energy Lab [6] was originally created to study passive solar heating systems, presently the software is also used to model solar energy applications. iHOGA by University of Zaragoza [7] is a C++-based software tool that exploits genetic algorithm for the multi-objective optimization of hybrid power systems. HYBRID2 by WEC-MIT [8] is a probabilistic/time series computer model that uses statistical methods to perform long-term economic analyses on various off-grid power system architectures. SAM by NREL [9] makes performance and cost of energy estimates for grid-connected power systems. It runs system simulations over a one-year period, in time steps of one hour, in order to emulate the performance of the system. PVsyst by PV syst SA [10] is a software for the study of stand-alone and grid-connected solar systems. It performs hourly simulation of the plant importing weather data form different sources as well as user-defined data.

However, the above methodologies and software do not consider some of the most important features of the rural electrification processes. Load consumption uncertainties are typically not evaluated, similarly no load evolution scenarios are investigated; this might have a strong impact on the microgrid design. Energy sources intermittent behavior needs for a proper modeling, and weather conditions have to be realistically estimated; several databases and models are available to support the designer's task [11–13]. Finally, in this paper authors want to enhance the crucial role of the storage equipment in off-grid systems [14]. System reliability and costs depend mainly on BESS performance and lifetime. Off-grid systems design procedures should implement accurate BESS models to embrace the unconventional working conditions in DCs scenarios and provide reliable results. The above-mentioned commercial software are based on simple BESS models (analytical approaches are the most adopted) since they can provide acceptable results in short time. TRNSYS adopts the Shepherd model [15] for lead-acid batteries; Shepherd model is the reference choice also by SAM but with the modification proposed by Tramblay [16]. HOMER and HYBRID2 adopt the KiBaM model both for lead-acid and Li-ion batteries. Finally, iHOGA proposes different options to users for lead-acid batteries: KiBaM, Shepherd model with modifications proposed by Copetti [17] and Schiffer model [18], moreover it includes also three models for Li-ion batteries. No commercial software attempts to compare different BESS modeling approaches for the sizing process of off-grid systems. Models based on stochastic, electric and electrochemical approaches have not been investigated and implemented.

Therefore, comprehensive procedures that couple the atypical features of rural contexts by including estimation errors into the design phase with proper components models are strongly required. For this reason, the next sections present a methodology for the robust design of off-grid electric power systems that consider both the uncertainties due to the rural context and the impact of different BESS models. This methodology has been already described and validated with respect to the robust design of a PV-BESS system [19]. In this paper, the attention is dedicated to developing suitable BESS models to be included in the procedure. Several modeling approaches (i.e., empirical and electrical) will be compared and exploited to simulate the microgrid behaviors. The final aim is to evaluate the BESS models impact on the microgrid design.

2. The Method of Analysis

This section introduces and summarized in three parts the whole procedure that addresses the off-grid power system design. The methodology, detailed and validated in [19], has been implemented

in a tool, namely Poli.NRG (POLItecnico di Milano—Network Robust desiGn). The tool is public available on [20].

- Data inputs gathering and processing—All the necessary information regarding users' electric needs, fixed and variable equipment costs and weather data are collected and processed to obtain load and sources profiles. Specifically, lifetime load profiles are obtained by means of Poli.NRG (LoadProGen subroutine [21]) that can formulate different realistic daily load profiles starting from field data [22]. Renewable source profiles are formulated according to specific models obtained from weather stations or from databases [23,24].
- System modeling and simulation—The operations of the specific off-grid power system are simulated over the plant lifetime according to specific components' and dispatch strategies models. In the case of a PV+BESS-based microgrid, the main components that must be modeled are PV generator, BESS and inverter [25,26]. The estimation of the PV energy output for each time-step k can be computed considering solar radiation profile, the size of the plant and the balance of system efficiency η_{BOS}, which embraces all the losses not directly related to the sun energy conversion process. The inverter size is defined according to the power peak occurring within the load profile and considering the inverter efficiency (η_{Inv}). Storage system is considered crucial for the off-grid system design and it can be modeled with different degree of details; empirical and simplified electric models of BESS are hence included as options in the Poli.NRG tool. Section 3 is dedicated to detail the modeling approaches used for BESS.

  For a given load curve LC and for given combinations of PV and BESS sizes, Poli.NRG provides techno-economic performance parameters (i.e., Loss of Load Probability, Net Present Cost and Levelized Cost of Energy) as output. Looking at the simulation process, for each time-step k, the difference between photovoltaic energy production $EPV(k)$ and load consumption $LC(k)$ represents the amount of energy that should be fulfilled by the BESS (charging or discharging):

$$\Delta E(k) = E_{PV}(k) - \frac{LC(k)}{\eta_{inv}} \tag{1}$$

  In real-life application, constraints are present which limit the BESS working conditions.

  First, BESSs must respect technological constraints like the maximum allowable power (defined by its EPR_{max}: maximum Energy Power Ratio). Consequently, the maximum energy that can be fluxed by the BESS in the given time-step k is computed as:

$$\Delta E^{max}_{BESS}(k) = \frac{BESS_{size}}{EPR_{max}} \cdot \Delta t \tag{2}$$

  For instance, if the EPR_{max} is 0.5 and the $BESS_{size}$ is 1 kWh, the battery can provide or accept a maximum injection of 2 kW. According to this limit the energy that flow through the BESS is evaluated as:

$$\Delta E_{BESS}(k) = \begin{cases} \Delta E(k) & \text{if } \Delta E(k) \leq \Delta E^{max}_{BESS}(k) \\ \Delta E^{max}_{BESS}(k) & \text{if } \Delta E(k) > \Delta E^{max}_{BESS}(k) \end{cases} \tag{3}$$

  Secondly, BESSs must respect their physical limits. Depending on the BESS modeling approach adopted (detailed in Section 3), these limits can be the maximum/minimum SoC levels or the maximum/minimum voltage levels.

  In discharge condition, BESS limitations can result in an amount of load that remains unsatisfied because the system is unable to supply it (assuming PV unavailability). This energy is represented by the Loss of Load (LL) indicator and it is computed as follows:

$$LL(k) = LC(k) - |\Delta E_{BESS}(k)| \text{ if } \Delta E_{BESS}(k) < 0 \tag{4}$$

For each simulation the system reliability is considered by computing the Loss of Load Probability LLP, which is the share of the electricity demand not fulfilled by the power system over its lifetime (LT) [27,28]:

$$LLP = \frac{\sum_{k=1}^{LT} LL(k)}{\sum_{k=1}^{LT} LC(k)} \quad (5)$$

Then the Net Present Cost (NPC), which is defined as the present value of the sum of discounted costs that a system incurs over its lifetime, is calculated [29]:

$$NPC = BESS_{size} \cdot C_{BESS} + \sum_{y=1}^{LT} \frac{O\&M(y) + C_R(y)}{(1+r)^y} - RV(LT) \quad (6)$$

where the first term of the sum is the initial investment cost that is proportional to the installed capacity $BESS_{size}$ given the specific cost of BESS C_{BESS}, the second term represents the sum of the net cash flows during each year y actualized with the expected discount factor r ($O\&M(y)$ are the operation and maintenance costs, while $C_R(y)$ accounts for replacement costs of BESS by taking into account the projected BESS cost at the specific year y), the third term $RV(LT)$ represents the residual value of the assets (i.e., BESS) at the end of the expected plant lifetime LT.

The Levelized Cost of Energy ($LCoE$) is also computed since it is a convenient indicator for comparing the unit costs of different technologies over their life, and it is a reference value for the electricity cost that rural consumers would face [30,31]. Moreover, it has also been employed as objective function in several analyses that deal with renewable-based off-grid power systems (e.g., [32–34]):

$$LCOE = \frac{r \cdot (1+r)^T}{(1+r)^T - 1} \cdot \frac{NPC}{(1 - LLP) \cdot \sum_{k=1}^{LT} LC(k)} \quad (7)$$

- Output formulation—A heuristic optimization method based on the imperialistic competitive algorithm [35] has been developed to manage the microgrid robust design. This method compares the techno-economic performances (LLP and NPC) of different combination of components' sizes in an iterative way. The optimal solution is the specific combination of components' sizes (PV_{opt} ; $BESS_{opt}$) which has the minimum NPC value while fulfilling the desired level of LLP [25].

  Once the optimal combination of components' sizes for a specific load profile is defined, the same heuristic procedure is repeated for other profiles within the same scenario. The new optimum points are likely to be different because of the different load profiles, hence the optimum points create a set of solutions instead of a single deterministic solution. The most robust solution (PV_{rbt}; $BESS_{rbt}$) within the set of solutions is computed as the most frequent solution among the obtained optimal solutions. New lifetime load profiles are tested till the following convergence criteria are satisfied:

$$\frac{\sigma(PV_{rbt}(n-1)) - \sigma(PV_{rbt}(n))}{\sigma(PV_{rbt}(n-1))} \leq \epsilon_{conv} \quad (8)$$

$$\frac{\sigma(BESS_{rbt}(n-1)) - \sigma(BESS_{rbt}(n))}{\sigma(BESS_{rbt}(n-1))} \leq \epsilon_{conv} \quad (9)$$

  where $(\sigma(PV_{rbt}(n)); \sigma(BESS_{rbt}(n)))$ indicates the standard deviations of the robust solution given the new n simulated profiles.

3. Novel BESS Models Proposed for a Proper Microgrid Design

For application of BESS within electrification approaches in DCs, selecting the best technology in terms of performance and durability is not the top priority: cost and availability on site play a relevant role in the final decision. The battery technology choice is usually defined by the economic capacity of the donor or investor. Thus, lead-acid batteries (in particular VRLA), which have benefited of years

of development with inevitably cost reduction and global spread, still represent the most common choice for all the applications (Solar home systems, mid-size PV systems, microgrid, and grid-ties back-up systems) [36,37]. As regards lithium batteries, they are rarely seen in DCs applications despite leveraged kWh costs of Li-ion BESS are comparable to lead-acid batteries (when considering the higher depth of discharge, lifetime and number of cycles) [38]. The initial investment cost is a barrier for both investors and donor agencies. However, due to the current experienced reduction in the overall cost of lithium-ion technology [39], it is presumable to forecast that Li-ion BESS will have a relevant share in the sector of off-grid system in the near future.

In such a contest, in this work, Li-ion is chosen as technology of reference for the BESS modeling phase within the adopted methodology for the robust design of off-grid power systems. Two main tasks are identified for battery models: the estimation of the operating conditions (i.e., SoC estimation), the estimation of the ageing (i.e., State of health (SoH) estimation). Two different BESS modeling approaches are considered: empirical and electrical. Empirical models are based on an abstract vision of electrochemical devices. The battery is described by a few analytical equations which do not consider the electrochemical processes behind, but they are empirically fitted. These models usually focus on the evaluation of the SoC of the battery based on energy balances. Electrical models focus on the electrical properties of a battery. An equivalent electric circuit is used to represent the battery dynamics by reproducing voltage and current characteristics at the external terminals. These models could be very simple, with few circuital elements, or more complex, with each circuital element related to a precise physical phenomenon occurring in the cell. These models are computationally more expensive than empirical models, but they can reach a higher degree of accuracy.

Specifically, two different empirical models (model 1 and model 2) are compared with one electrical model (model 3). In all the cases, BESS models have to fulfil the energy balance $\Delta E(k)$ between production (PV) and demand (load) and update the State of Charge (SoC) and State of Health (SoH) indicators. The differences lie in the way in which the SoC and SoH are estimated (i.e., the modeling approach). Eventually, these differences will result in marked deviations in LLP and NPC estimations, impacting on the final design evaluation. The models have been developed within the framework of the collaboration between the Politecnico di Milano (DoE department) and CSEM-PV-Center (Swiss Center for Electronics and Microtechnology). All the measurement was performed at the Energy Storage Research Center (ESReC) located in Nidau (CH) on the Li-ion LNCO cell from Boston Power SWING5300 and then extended at the system level for the purpose of the analyses of the present work [40].

3.1. Empirical Models

In the empirical model, BESS is modeled as an ideal storage system. Main features are the SoC limits (SoC_{min} and SoC_{max}), charge (η_C) and discharge (η_D) efficiencies, minimum SoH (SoH_{min}) and capacity fade index cf (i.e., the loss of SoH per cycle). Moreover, the energy stored in the battery needs to be updated based on the amount previously stored ($E_{BESS}(k-1)$) as follows:

$$E_{BESS}(k) = \begin{cases} E_{BESS}(k-1) + \Delta E_{BESS}(k) \cdot \eta_C & \text{if } \Delta E_{BESS}(k) > 0 \\ E_{BESS}(k-1) + \frac{\Delta E_{BESS}(k)}{\eta_D} & \text{if } \Delta E_{BESS}(k) < 0 \end{cases} \quad (10)$$

On this point, the two proposed empirical models are differentiated as regards of the efficiency values:

- Model 1 assumes a fix value of round-trip efficiency $\eta_{RT} = 95\%$ as claimed in the literature and/or manufacturers data for similar studies [41]. Charge and discharge efficiency can be derived considering symmetry in charge/discharge processes so that $\eta_C \cdot \eta_D = \eta_{RT}$.
- Model 2 assumes a variable value of efficiency linked to the operating rate (In a battery system, the operating rate is usually represented by the C-rate that is the ratio between the actual current and the nominal capacity. For the purpose of this paper, C-rate is approximated by

the E-rate=$(\Delta E_{BESS}(k)/\Delta t)/BESS_{size}$) during the specific time-step k. The adopted function is derived from experimental tests and shown in Figure 1.

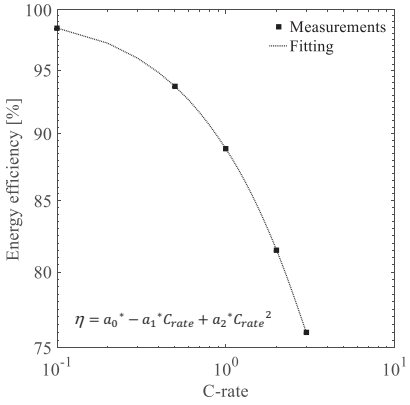

Figure 1. Efficiency of the LNCO Li-ion cell BOSTON POWER SWING 5300 measured at ambient temperature with symmetric charge-discharge cycles at different C-rates (DoD = 100%) [42].

Then, the new state of charge (SoC) is computed based on the previous value:

$$SoC(k) = \frac{E_{BESS}(k)}{BESS_{size} \cdot SoH(k-1)} \tag{11}$$

where $SoH(k-1)$ represents the assumed ageing state of the BESS during times step k (SoH computation is detailed in Section 3.3). In this modeling approach, the maximum energy that can be absorbed or provided by the battery ΔE_{BESS} is limited by the SoC limits: SOC_{min} and SOC_{max}. If $SOC(k) > SOC_{max}$ a part of ΔE_{BESS} in Equation (10) is not exploited to charge the battery. In the same way, if $SOC(k) < SOC_{min}$ a part of ΔE_{BESS} generates a loss of load (Equation (4)).

3.2. Electrical Model

Electrical models can reproduce the full battery dynamics using equivalent electric circuits. There is a wide range of circuital models, with a different degree of complexity. The use of very complex electrical models like the one proposed in [43] or [44] within the proposed methodology is not suitable since it can bring to expensive computational effort. For this reason, simplified electrical models represent an appropriate compromise. Therefore, the proposed Model 3 is a simplified electrical model made by two circuital elements: the R-C series circuit of Figure 2.

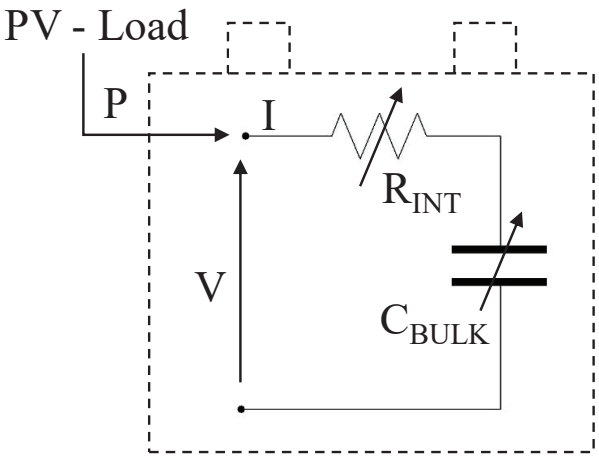

Figure 2. Simplified electrical model for electrochemical cell adopted in the proposed methodology.

Specifically:

- C_{BULK} is a capacitor of big-variable capacitance called incremental, differential or intercalation capacitance [44,45]. The voltage drop at the terminals of this element represents the open circuit voltage (OCV) behavior and hence the SoC estimation [46]. Figure 3a shows the trend of C_{BULK} in fresh cell condition which has been derived from OCV measurements (i.e., discharge curve at very low current: C/100) and adopted in the simulations. This curve is commonly called *IC curve*, referring to the Incremental/Intercalation Capacity.
- R_{INT} is a resistor that models the cell over-potential in regime conditions. It represents the equivalent resistance of the cell at a characteristic stress frequency that depends on the typical BESS working conditions. The resistance has been measured in the lab at a frequency correspondent to the time-step of the procedure adopted. Poli.NRG is based on load and generation profile defined with a time-step equal to 1 min ($\Delta t = 60s$): the simulated BESS injections will have a fundamental frequency of 16 mHz. Consequently, the Resistance R_{INT} has been mapped at this frequency and different SoCs as shown in Figure 3 (fresh cell condition and quadratic fitting function have been assumed).

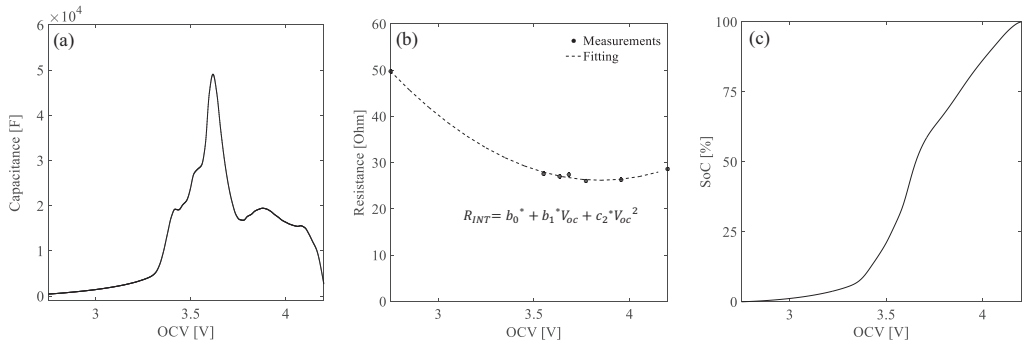

Figure 3. Model parameters measured at ambient temperature for the LNCO Li-ion cell BOSTON POWER SWING 5300 at different OCV (i.e., SoC) [46]: (**a**) intercalation capacitance C_{BULK}; (**b**) equivalent resistance at 16 mHz R_{INT} and correspondent fitting function; (**c**) OCV-SOC relationship derived from OCV measurements.

The current flowing through the electrical cell model has been assumed equal to:

$$I(k) = \frac{\frac{\Delta E_{BESS}(k)}{\Delta t}}{V(k) \cdot \frac{BESS_{size}}{E_{n,cell}}} \tag{12}$$

where the ratio at the denominator represents the number of equivalent cells inside the BESS, obtained dividing the total capacity of the battery $BESS_{size}$ by the nominal capacity of a single cell $E_{n,cell}$. The number of cells is used as the scaling factor to shift the calculations at cell level.

The open circuit voltage $V_{oc}(k)$ and $V(k)$ can be updated at instant k by accounting for the capacitance value C_{BULK} and R_{INT} at the previous time-step:

$$V_{oc}(k) = V_{oc}(k-1) + \frac{I(k)}{C_{BULK}(k-1, V_{oc}(k-1))}\Delta t \tag{13}$$

$$V(k) = V_{oc}(k) + R_{INT}(k-1, V_{oc}(k-1)) \cdot I(k) \tag{14}$$

$SoC(k)$ indicator is directly derived from $Voc(k)$ as detailed in Figure 3c. Ageing is accounted by C_{BULK} and R_{INT} parameters: SoH and State of Resistance (SoR) indicators are used to update both parameters during lifetime (SoH and SoR computation is detailed in Section 3.3).

In this modeling approach, the maximum energy that can be absorbed or provided by the battery ΔE_{BESS} is limited by the voltage limits: V_{min} and V_{max}. If $V(k) > V_{max}$, ΔE_{BESS} in Equation (10) is

not exploited to charge the battery. In the same way, if $V(k) < V_{min}$, ΔE_{BESS} generates a loss of load (Equation (4)). A more realistic behavior of the battery is considered compared to the limit of the empirical models.

3.3. Ageing Modeling

Beside the SoC estimation approaches for the considered models, BESS models should also be able to represent degradation during cycling (i.e., capacity fade and power fade effects). Understanding of the chemical and physical processes that lead to battery ageing is critical in optimizing battery usage, lifetime, chemistry and construction [47]. The issue is very challenging due to the large number of possible reactions and the interactions of these, along with the highly limited possibilities of collecting data during operation of the battery. In the literature, different degree of details is provided especially when dealing with capacity fade modeling. In [48,49] a cycling counting model is corrected by using a simplified power function which correct the cycle numbers regarding the depth of discharge (DoD) of each cycle. In [50] a more comprehensive ageing model is proposed which analytically correlate the capacity fade with the main ageing factors: cycling rate, DoD and temperature. In this work, all the previously presented BESS models (both empirical ones and electrical ones) accounts for ageing phenomena but with different degree of details: from a purely measurement-independent approach to a fully detailed model closely linked to the experimental results. Ageing studies are time intensive and usually only focus on one or two chemistries and a few ageing conditions. They are therefore not providing a complete understanding of the entire range of temperatures and state of charges. In [51] a wide review is provided on the Li-ion ageing research of commercially available batteries with different cathode and anode chemistries. In the proposed BESS models, ageing phenomena are taken into account in both empirical and electrical models. First, the cycles number registered during the time-step is computed as follows

$$cy(k) = \left| \frac{SoC(k) - SoC(k-1)}{2} \right| \tag{15}$$

where $cy(k)$ is the equivalent cycle during time-step k. The cumulate function of cy accounts for the cycles till time-step k. SoH can be then updated with the following equation:

$$SoH(k) = SoH(k-1) - cy(k) \cdot cf(k) \tag{16}$$

when $SoH(K) = SOH_{min}$ the battery is assumed to be exhausted and replaced and C_R in Equation (6) is updated. As regards of the capacity factor (cf) (i.e., the loss of capacity per cycle), the three models are differentiated:

- Model 1 assumes constant cf that is based on the maximum number of cycles as claimed in the literature and/or manufacturers data for similar studies [52].

$$cf(k) = \frac{1 - SoH_{min}}{cy_{max}} \tag{17}$$

  For instance, if cy_{max} = 5000 and SoH_{min} = 80%, cf will results in 0.004%/cycle.
- Model 2 and Model 3 assume a variable value of cf that is linked to the operating condition, and in particular to the C-rate (Figure 4a).

In general, degradation is modeled differently among the proposed models:

- Model 1 and Model 2: use SoH to update the available energy (i.e., capacity fade) as showed in Equation (11).

- Model 3: R and C parameters are updated each time-step. The IC curve of Figure 3a is scaled proportionally to SoH indicator accounting for the capacity fade:

$$C_{BULK}(k) = C_{BULK} \cdot SoH(k) \tag{18}$$

while the resistance function of Figure 3 is multiplied by the State of Resistance (SoR) indicator that account for the resistance increase at the time-step k (i.e., power fade):

$$R_{INT}(k) = R_{INT} \cdot SoR(k) \tag{19}$$

$$SoR(k) = SoR(k-1) + cy(k) \cdot rf(k) \tag{20}$$

where rf is the resistance increasing factor that depends on the operating condition during the specific time-step k. rf is hence computed each time-step by following the expression in Figure 4b.

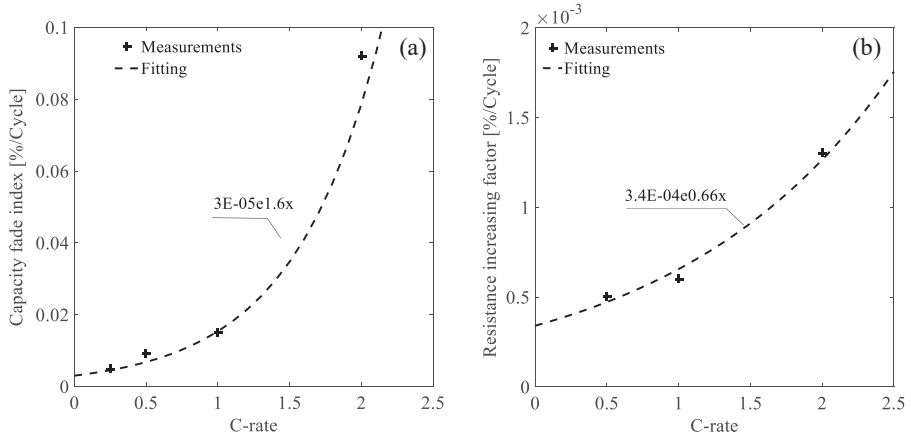

Figure 4. Capacity fade index cf (**a**) and resistance increasing factor rf (**b**) as function of C-Rate. The trends have been measured using the cycling procedure presented in [46].

Table 1 resumes the main assumptions of the three models adopted in the simulations.

Table 1. Main characteristics of the BESS models adopted in the proposed methodology.

Model	SoC Estimation	SoH Estimation
Model 1 - Empirical (FIX)	SoC limits $\eta_{RT} = 95\%$	$SoH_{min} = 80\%$ cf = fix cy_{max} = fix
Model 2 - Empirical (VAR)	SoC limits $\eta_{RT} = f$(C-Rate)	$SoH_{min} = 80\%$ $cf = f$(C-Rate)
Model 3 - Electrical	Voltage limits $R_{INT} = f$(SoC, SoR) $C_{BULK} = f$(SoC, SoH)	$cf = f$(C-Rate) $rf = f$(C-Rate)

4. The Case Study

The methodology of Section 2 with the different BESS models detailed in Section 3 have been implemented in the tool Poli.NRG and they have been used to run different sets of simulations which are detailed in the following.

The procedure has been applied to design a microgrid, based on PV generators coupled with BESS lithium-ion technology, to supply power to the Ngarenanyuki Secondary School (Tanzania). This school was targeted by the project Energy4Growing [20] and it is a suitable test bed for the

procedure since electrical data related to the school are available thanks to the monitoring system in place.

Thanks to a specific survey, electric needs of the Ngarenanyuki school have been collected. Data about the number and the type of appliances in use, their nominal power, and some qualitative information about users' behavior with respect to each appliance are organized and used as input for the Poli.NRG procedure (LoadProGen subroutine). Different possible realistic lifetime load curves are generated to be used in the simulations according to an evolution scenario that considers the load to increase with a constant rate (1%/year).

As regards of the solar resource, approach validated in [53] and the available dataset published in [23] have been used for the simulations. The method employed can take into accounts the variability of the solar resource throughout the year. For instance, lower values of irradiation are expected in February and November, in correspondence to the rainy seasons.

Technical and economical parameters in the simulations are reported in Table 2. Cost information about PV modules, batteries, and off-grid inverters are the result of a survey among Tanzanian local suppliers, while O&M, other investment costs and modeling parameters (efficiencies mostly) have been estimated based on experience. For each single lifetime profile and scenario, the optimal PV-BESS is defined as the one with the minimum NPC, respective a maximum LLP of 5%.

Table 2. Parameters adopted in the simulation with Poli.NRG tool.

Parameter	Parameter Name/Note	Value
Economics		
Plant lifetime	LT	20 y
LLP target value	% of total load	5%
PV modules cost	Monocrystalline	2500 €/kWp
Battery cost (replacement)	Lithium-ion	[39]
Off-grid inverter cost	-	900 €/kW
Other investment costs	% on the main component costs	20%
O&M cost	-	100 €/kWh
Discount rate	r	6%
Components		
Balance of system efficiency	η_{BOS}	85%
Inverter efficiency	η_{Inv}	90%
BESS—Minimum SoH	SoH_{min}	80%
BESS—Maximum lifetime	$LT_{BESS,max}$	10 y
BESS—Max Energy to Power Ratio	EPR_{max}	0.5
BESS(M1)—Round-trip efficiency	η_{RT}	95%
BESS(M1)—Maximum number of cycles	cy_{max}	Variable
BESS(M1-M2)—Minimum SoC	SoC_{min}	0%
BESS(M1-M2)—Maximum SoC	SoC_{max}	100%
BESS(M3)—Minimum cell Voltage	V_{min}	2.75 V
BESS(M3)—Maximum cell Voltage	V_{max}	4.2 V
Simulation Settings (Opsim Tool)		
Load increasing rate		1%/year
Convergence criterion	ϵ_{conv}	0.5%
PV step size	PV_{step}	0.05 kW
PV range	$PV_{min} \div PV_{max}$	0 ÷ 6 kW
BESS step size	$BESS_{step}$	0.05 kWh
BESS range	$B_{min} \div B_{max}$	0 ÷ 35 kWh
BESS(M1-M2-M3)—Starting SoH	SoH_{start}	100%
BESS(M1-M2)—Starting SoC	SoC_{start}	100%
BESS(M3)—Starting Open Circuit Voltage	$V_{oc,start}$	4.2 V
BESS(M3)—Starting SoR	SoR_{start}	100%

5. Simulations, Results and Discussion

In this section, the results obtained by different simulations of the study case with Poli.NRG tool are presented. Specifically, the discussions will be focused on two different layers of analysis:

1. Microgrid simulation with different BESS models. A detailed comparison between empirical (M1 and M2) and electrical (M3) BESS models is presented. As regards of the BESS empirical M1, two different values for the maximum number of cycles (cy_{max}) are tested: (i) M1-1 uses $cy_{max} = 10,000$ to reproduce the highest value claimed in the literature for Li-ion technology and (ii) M1-2 uses $cy_{max} = 3000$ which represents a more reliable data that belongs to the Li-ion LNCO chemistry [40]. Simulations will demonstrate the high impact of BESS modeling approach on SoC and SoH estimations.
2. Microgrid robust design. The focus is on the microgrid robust design as proposed in the presented procedure, results will show how different BESS models lead to different optimal plant configuration.

5.1. Microgrid Simulation with Different BESS Models

The first level of analysis has been focused on the comparison of the different BESS models within the novel procedure for the robust design of off-grid systems. Different plant configurations have been selected and simulated with Poli.NRG. The PV size is fixed to 4 kW while the BESS is considered in three sizes: SMALL (1 kWh), MEDIUM (10 kWh) or LARGE (100 kWh). Figure 5 shows the impact of these hypotheses. A one-month winter scenario (February) is considered in the figure since it is characterized by high variability in the solar resources. The power to be delivered by the BESS is the same for the three simulated plants; however, the operating rate (E-rate) is higher for the SMALL BESS (blue line) and lower for the LARGE BESS (red line for MEDIUM and yellow line for the LARGE one). Higher E-rates will result in higher replacement costs making the hypothesis not convenient from a techno-economic point of view; vice-versa, the biggest the BESS capacity the higher the investment costs. This motivates the procedure proposed and implemented in Poli.NRG that looks at the best plant configuration that satisfy a predefined level of LoL at the minimum NPC.

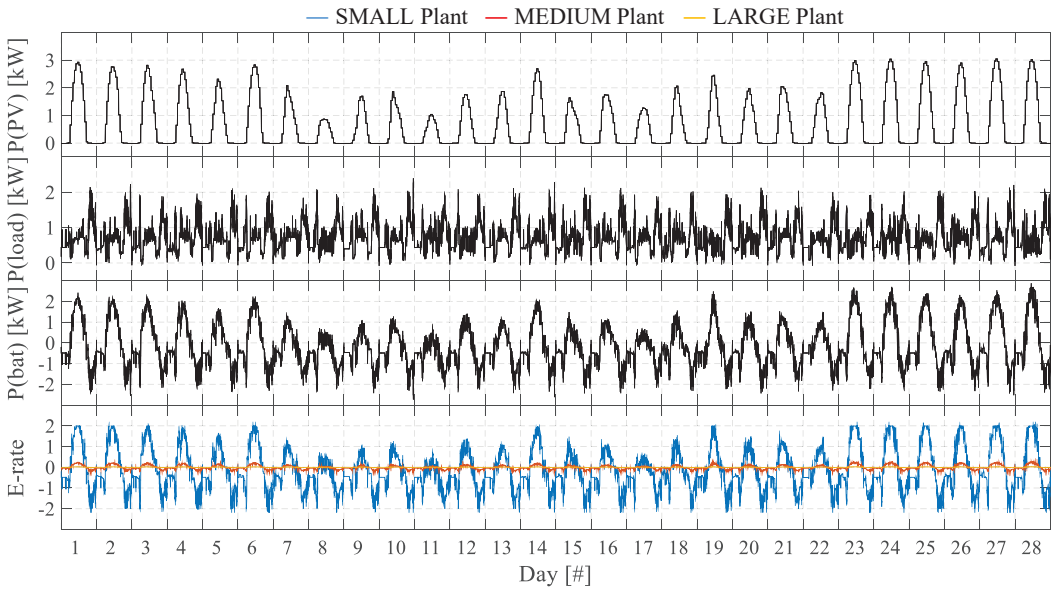

Figure 5. Simulation results for the month of February of year 1: assumed photovoltaic and load power profiles, simulated BESS power profile and operating rate.

Figure 6 shows the simulated SoC for the four different BESS models proposed within the three hypotheses of plant configuration. The two empirical M1 (black and blue lines), which represent

BESS with fix efficiency and a fix number of maximum cycles cy_{max} (M1-1:10,000 or M1-2:3000), are overlapped: differentiation will emerge due to ageing and hence simulating the plant for several years. The empirical M2 (green line), which is characterized by variable efficiency and lifetime according to the operating conditions, distinguishes from M1 in case of MEDIUM/LARGE plants. It results that M1 overestimates the discharge profile: the assumed constant efficiency is probably too severe, and it does not take into account the specific operating condition. This is a limitation of simplified models which use literature data and datasheet to set model's parameters. Special case in the one of SMALL plants in which M1-1, M1-2 and M2 saturate to the limits because of the high operating rate, then hiding the differences in SoC estimations. In general, this is a limitation of all empirical models which do not account for technological limitations (i.e., voltage limits). Conversely, electrical model M3 (red line) differs from empirical models. Charging phases stops at low level of SoC due to overcome voltage limits. The same happens in discharge phases thus affecting LoL estimation. This fact differentiates the simulation achievable with electrical model if compared to empirical models.

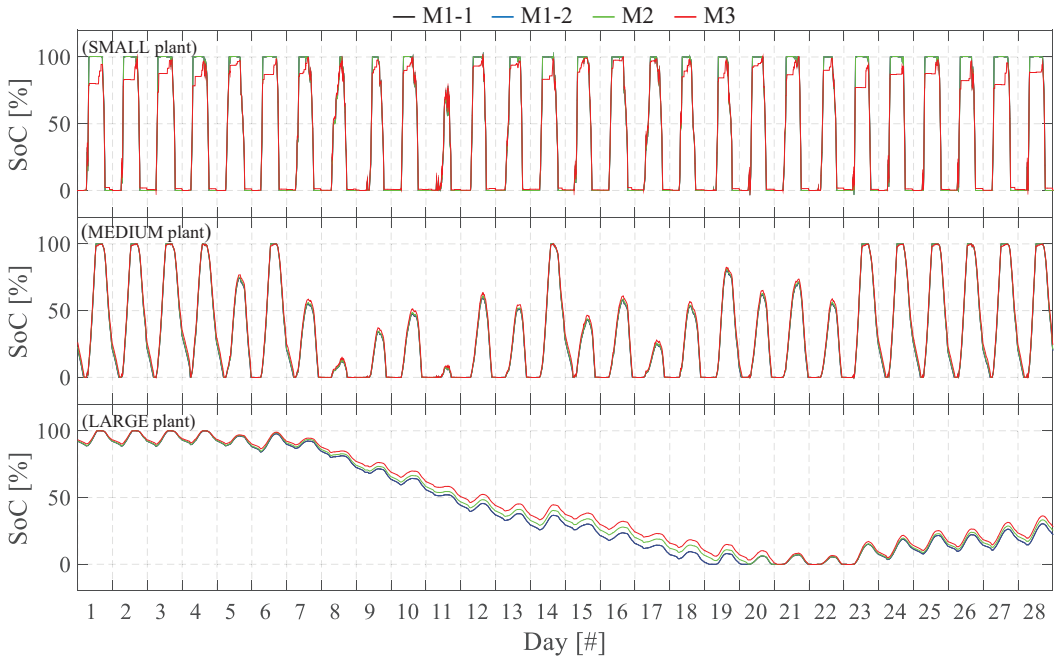

Figure 6. Estimated SoC trends for the month of February of year 1 with different BESS models.

Figure 7 shows SoH trends along the plant lifetime. Sudden changes in the SoH indicator highlight replacements during years. In this case, M1-1 and M1-2 differentiate due to the different cy_{max}. Higher cy_{max} (M1-1) means less replacements. Empirical models that relate SoH estimation only on a maximum number of cycles as per Equation (17) without considering cycling conditions, may end up in wrong SoH estimations. This fact is confirmed in case of SMALL plants (undersized BESS) for M1-1: albeit operating rate is so stressful (high E-rate in Figure 5) it is not impacting on BESS replacements. Consequently, replacement is only based on reached maximum lifetime $LT_{BESS,max}$. This is not the case of the model M1-2 where the assumption of cy_{max} = 3000 significantly increases replacements. In other words, empirical models totally rely on assumptions about BESS aggregated parameters (i.e.,: efficiency and maximum cycle numbers), which should be carefully defined with respect to the final application. These problems are not present in the case of M2 and M3 because they account for the cycling rate in the ageing estimation. Apart from SMALL plant, these two models provide very similar SoH estimation (red and green line are almost overlapped): capacity fade is in fact derived from the same set of measurements (Figure 4).

All the above findings, about SoC and SoH estimations, impact on the LoL estimations as showed in Table 3. Differences emerge in the simulation of MEDIUM and LARGE plants. M1-1 (cy_{max} = 10,000)

results in a lower LoL if compared to M1-2 (cy_{max} = 3000) and this is due to higher capacity fade of the latter case: a lower capacity will indeed affect the LoL negatively. M3 results in the lowest values in all the three hypotheses. Given the higher accuracy provided by electrical model, it results that empirical models tend to overestimate LoL. This fact can be explained by the totally different approaches used to describe battery behaviors between empirical and electrical models: the first one makes use of energy/power balances to compute SoC, while the second one uses electrical quantities (i.e., voltages/currents) to derive SoC. This clearly affects the charge/discharge paths that in the end result into different LoL indicators.

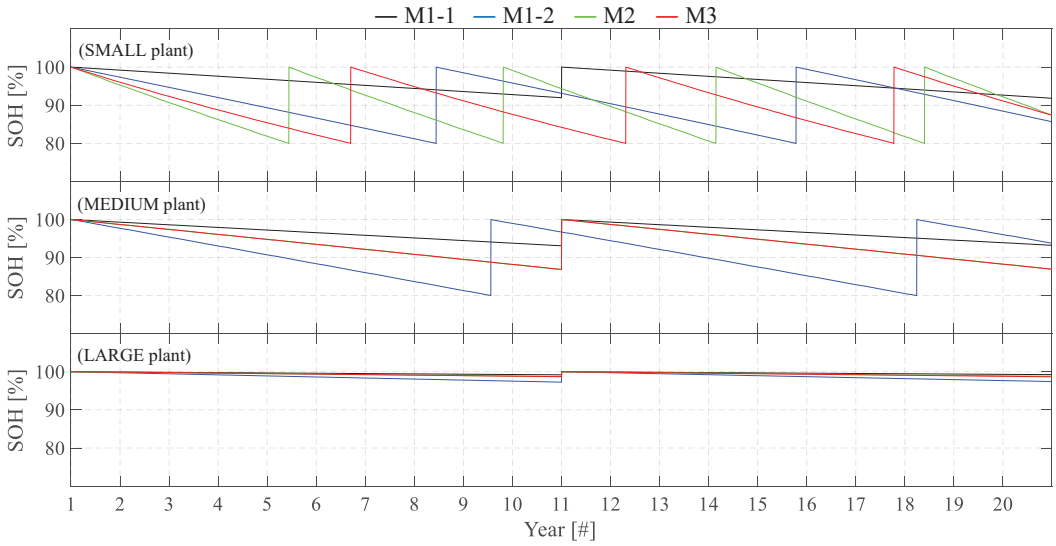

Figure 7. State of health degradation considering different BESS models.

Table 3. Simulation results about LoL estimation with different BESS models.

LoL [%]	M1-1	M1-2	M2	M3
SMALL plant	56.56	56.81	56.93	56.91
MEDIUM plant	18.18	20.18	18.69	18.16
LARGE plant	9.78	9.78	7.85	7.19

5.2. Microgrid Robust Design

Given the results obtained by simulating different plant configurations, the second level of analysis has been focused on the robust design of the case study. Poli.NRG tool, improved with the new energy storage models, has been used to simulate the different load curves and to find the optimal plant configuration for each of them. Figure 8 and Table 4 show the obtained results in terms of sets of solutions. Each set of solution is related to a specific BESS modeling approach. In case of M1 models, around 90 LCs (each one detailed in a 20 years profile at 1 min time-step) are needed before reaching convergence, while M2 and M3 need less LCs: 42 and 62, respectively. The most frequent configuration within the simulated LCs indicates the most robust solution (PV_{rbt}; $BESS_{rbt}$). f_{rbt} parameter indicates how many times the robust solution resulted to be the optimal solution for a specific model. PV optimal size is almost the same (4.10–4.15 kW) in all cases, being closely linked to the solar resources rather than the BESS models. BESS optimal size is instead influenced by the modeling approach. Results depict that BESS should range around 13.70–16.20 kWh with a maximum variation of 18%. Empirical models of type M1 tend to oversize the plant, especially if wrong assumptions about cycling conditions (see M1-1) are made. On the contrary, empirical model of type M2 and the electrical model M3 provide very similar results (i.e., the same PV size and the 2% of difference in between the BESS sizes). Economics are also influenced by the adopted BESS model. NPC and LCoE are computed as the average value among the f_{rbt} simulated LCs that resulted in having the robust solution as the optimal one. Overall, NPC and

LCoE for the robust plant configuration are around 34 k€ and 0.47 €/kWh respectively. In general, LLP and NPV estimations of model M3 are surely preferable because capacity fade and power fade are the results of capacitance and internal resistance variations: BESS dynamic and ageing behaviors are linked to physical phenomena. But this comes at the price of a considerably higher computational effort: M3 is 14 times slower that M1 and 4 times slower than M2. Therefore, in planning tools like Poli.NRG, modified empirical models which account for capacity fade by using simplified analytical curves (Figure 1) can represent a suitable compromise to obtain reliable results in a reasonable time (Simulation time based on Intel®Core™i7-4790 CPU 3.6GHz, RAM 16 GB.).

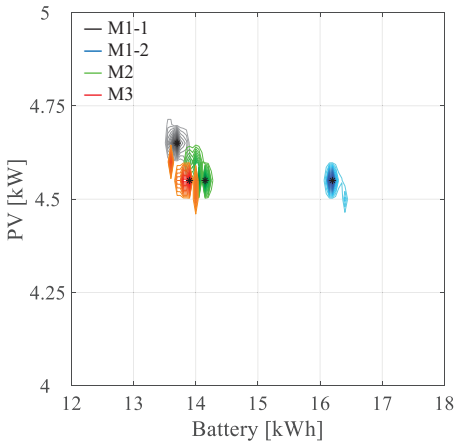

Figure 8. Area of solutions obtained by running the proposed novel procedure (Poli.NRG) over the Tanzanian study case with different BESS models.

Table 4. Robust design results obtained with different BESS models.

BESS Model	Simulation Time [s/LC]	Simulated LCs [numb]	Robust Solution					
			f_{rbt}	PV_{rbt} [kW]	$BESS_{rbt}$ [kWh]	NPC [k€]	LCOE [€/kWh]	LLP [%]
M1-1	640	92	29	4.65	13.70	33.8	0.471	5
M1-2	640	96	35	4.55	16.20	35.1	0.489	5
M2	2180	42	10	4.55	14.15	33.7	0.469	5
M3	8900	62	8	4.55	13.90	33.5	0.466	5

6. Conclusions

In this paper, a comprehensive methodology for the robust design of PV-BESS systems for rural electrification in Developing Countries (DCs) has been proposed. The attention has been dedicated to developing suitable BESS models to be included in the procedure: several modeling approaches (i.e., empirical and electrical) have been compared and simulated. With respect to the related literature, the hallmark of this methodology is the capability to incorporate the uncertainties inherent to rural electrification processes: load consumption uncertainties, load evolution scenarios, unpredictable energy sources and proper BESS models—able to appropriately represent State of Charge (SoC) and State of Health (SoH) indicators—have been determined as pivotal features to correctly evaluate the robust design of off-grid systems. Once a case study is selected, the system operations are simulated over the entire plant lifetime. The evaluation of the battery replacement costs, the Loss of Load Probability (LLP), the Net Present Cost (NPC) and the levelized cost of electricity are proposed as performance indices to rank the possible microgrid configurations. Several lifetime load profiles are simulated to find the optimal microgrid configuration to fulfil the desired LLP with the minimum NPC (i.e., heuristic optimization method). The methodology has been proposed in the form of a computational tool in MATLAB®named Poli.NRG (POLItecnico di Milano—Network Robust desiGn) and applied to size a PV+BESS microgrid system to supply power to a rural village of Tanzania.

The results showed that BESS models highly affect SoC and SoH estimations and thus LLP and NPC computations. Simplified empirical models, based on literature/manufacturers data might lead to oversized plant, especially if wrong assumptions about cycling conditions have been made. On the contrary, performance estimation made with electrical model has been shown to be preferable because degradation factors (capacity fade and power fade) are the direct results of model's parameters variations (capacitance and internal resistance variations). However, the higher accuracy comes at the expense of higher simulation time which increases by more than ten times. Therefore, modified empirical models which account for degradation factors (i.e., capacity fade) by including simplified analytical curves, instead of relying on manufacturers data, have been shown to represent a suitable solution to obtain reliable results with a viable computational effort. Overall, this paper has highlighted that attention is required when facing the design of off-grid power systems in DCs. Uncertainties on loads, generators and on the mathematical models adopted to simulate BESS behavior, could highly impact on the techno-economic evaluations.

Author Contributions: Conceptualization, M.M. (Matteo Moncecchi), C.B., S.M. and M.M. (Marco Merlo); Investigation, M.M. (Matteo Moncecchi), C.B., S.M. and M.M. (Marco Merlo); Methodology, M.M. (Matteo Moncecchi), C.B., S.M. and M.M. (Marco Merlo); Validation, M.M. (Matteo Moncecchi), C.B., S.M. and M.M. (Marco Merlo); Writing—original draft, M.M. (Matteo Moncecchi) and C.B.; Writing—review & editing, S.M. and Marco Merlo. All authors have read and agreed to the published version of the manuscript.

Funding: This research received no external funding.

Acknowledgments: We thank Vincenzo Musolino of the PV-Center CSEM SA for the support in the development of the electrical battery model.

Conflicts of Interest: The authors declare no conflict of interest.

Nomenclature

General	
DCs	developing countries
PV	photovoltaic
BESS	battery energy storage system
Poli.NRG	POLItecnico di Milano—Network Robust desiG
PV & Load Modeling	
$EPV(k)$	photovoltaic energy production at time-step k
$LC(k)$	load consumption at time-step k
η_{BOS}	balance of system efficiency
η_{Inv}	inverter efficiency
Bess Modeling	
$BESS_{size}$	capacity of the BESS
EPR_{max}	maximum Energy Power Ratio
C_{BULK}	incremental capacitance
R_{INT}	internal resistance
SOC	state of charge
SOH	state of health
SOR	state of resistance
$cy(k)$	equivalent cycle during time-step k
cf	capacity factor (i.e., the loss of capacity per cycle)
Investment Evaluation	
LT	Lifetime of the power system [years]
r	discount rate [%]
$RV(LT)$	Residual value of the asset at the end of the expected plant lifetime LT (€)
LLP	Loss of Load Probability [%]
NPC	Net Present Cost [€]
LCoE	Levelized Cost of Energy [€/kWh]

References

1. IEA. *World Energy Outlook 2014*; OECD Publishing: Paris, France, 2014; p. 690. [CrossRef]
2. Khatib, T.; Ibrahim, I.A.; Mohamed, A. A review on sizing methodologies of photovoltaic array and storage battery in a standalone photovoltaic system. *Energy Convers. Manag.* **2016**, *120*, 430–448. [CrossRef]
3. Sinha, S.; Chandel, S. Review of software tools for hybrid renewable energy systems. *Renew. Sustain. Energy Rev.* **2014**, *32*, 192–205. [CrossRef]
4. National Renewable Energy Laboratory (NREL). HOMER—Hybrid Renewable and Distributed Generation System Design Software. Available online: https://www.homerenergy.com/ (accessed on 31 March 2020).
5. CANMET. RETScreen International Home. Available online: https://www.nrcan.gc.ca/maps-tools-publications/tools/data-analysis-software-modelling/retscreen/7465 (accessed on 31 March 2020).
6. Thermal Energy System Specialists LLC. TRNSYS—Transient System Simulation Tool. Available online: http://www.trnsys.com/ (accessed on 31 March 2020).
7. University of Zaragoza. Software iHOGA—Improved Hybrid Optimization by Genetic Algorithms. Available online: https://ihoga.unizar.es/en/ (accessed on 31 March 2020).
8. Wind Energy Center—University of Massachusetts. Hybrid2 Software. Available online: https://www.umass.edu/windenergy/research/topics/tools/software/hybrid2 (accessed on 31 March 2020).
9. Blair, N.; Dobos, A.P.; Freeman, J.; Neises, T.; Wagner, M.; Ferguson, T.; Gilman, P.; Janzou, S. System Advisor Model, Sam 2014.1. 14: General Description. Available online: https://www.nrel.gov/docs/fy14osti/61019.pdf (accessed on 31 March 2020).
10. PVSyst S.A. PVSyst Photovoltaic Sofware. Available online: https://www.pvsyst.com/ (accessed on 31 March 2020).
11. IRENA. Global Atlas for Renewable Energy. Available online: https://www.irena.org/globalatlas (accessed on 31 March 2020).
12. NASA. Prediction Of Worldwide Energy Resources (POWER). Available online: https://power.larc.nasa.gov/ (accessed on 31 March 2020).
13. UE JRC's Directorate. Photovoltaic Geographical Information System (PVGIS). Available online: https://re.jrc.ec.europa.eu/pvg_tools/en/tools.html#PVP (accessed on 31 March 2020).
14. Mandelli, S.; Brivio, C.; Leonardi, M.; Colombo, E.; Molinas, M.; Park, E.; Merlo, M. The role of electrical energy storage in sub-Saharan Africa. *J. Energy Storage* **2016**, *8*, 287–299. [CrossRef]
15. Hussein, A.A.; Batarseh, I. An overview of generic battery models. In Proceedings of the 2011 IEEE Power and Energy Society General Meeting, Detroit, MI, USA, 24–28 July 2011; pp. 1–6. [CrossRef]
16. Tremblay, O.; Dessaint, L.A.; Dekkiche, A.I. A Generic Battery Model for the Dynamic Simulation of Hybrid Electric Vehicles. In Proceedings of the 2007 IEEE Vehicle Power and Propulsion Conference, Arlington, TX, USA, 9–12 September 2007; pp. 284–289. [CrossRef]
17. Copetti, J.B.; Lorenzo, E.; Chenlo, F. A general battery model for PV system simulation. *Prog. Photovolt. Res. Appl.* **1993**, *1*, 283–292. [CrossRef]
18. Schiffer, J.; Sauer, D.U.; Bindner, H.; Cronin, T.; Kaiser, R. Model prediction for ranking lead-acid batteries according to expected lifetime in renewable energy systems and autonomous power-supply systems. *J. Power Sources* **2007**, *168*, 66–78. [CrossRef]
19. Brivio, C.; Moncecchi, M.; Mandelli, S.; Merlo, M. A novel software package for the robust design of off-grid power systems. *J. Clean. Prod.* **2017**, *166*, 668–679. [CrossRef]
20. Politecnico di Milano. Energy4Growing. Available online: http://www.e4g.polimi.it/ (accessed on 31 March 2020).
21. Mandelli, S.; Merlo, M.; Colombo, E. Novel procedure to formulate load profiles for off-grid rural areas. *Energy Sustain. Dev.* **2016**, *31*, 130–142. [CrossRef]
22. Mandelli, S.; Brivio, C.; Colombo, E.; Merlo, M. Effect of load profile uncertainty on the optimum sizing of off-grid PV systems for rural electrification. *Sustain. Energy Technol. Assess.* **2016**, *18*, 34–47. [CrossRef]
23. Renewable Ninja. Available online: https://www.renewables.ninja/ (accessed on 31 March 2020).
24. SoDa—Solar Radiation Data. Available online: http://www.soda-pro.com/ (accessed on 31 March 2020).
25. Shen, W.X. Optimally sizing of solar array and battery in a standalone photovoltaic system in Malaysia. *Renew. Energy* **2009**, *34*, 348–352. [CrossRef]

26. Kaldellis, J.K. Optimum technoeconomic energy autonomous photovoltaic solution for remote consumers throughout Greece. *Energy Convers. Manag.* **2004**, *45*, 2745–2760. [CrossRef]
27. Jakhrani, A.Q.; Othman, A.K.; Rigit, A.R.H.; Samo, S.R.; Kamboh, S.A. A novel analytical model for optimal sizing of standalone photovoltaic systems. *Energy* **2012**, *46*, 675–682. [CrossRef]
28. Tsalides, P.; Thanailakis, A. Loss-of-load probability and related parameters in optimum computer-aided design of stand-alone photovoltaic systems. *Sol. Cells* **1986**, *18*, 115–127. [CrossRef]
29. Farret, F.A.; Simões, M.G. Micropower System Modeling with Homer. In *Integration of Alternative Sources of Energy*; Wiley-IEEE Press: Hoboken, NJ, USA, 2006; Chapter 15, pp. 379–418. [CrossRef]
30. IEA. Projected Costs of Generating Electricity. In *Projected Costs of Generating Electricity*; OECD Publishing: Paris, France, 2010; Volume 118, p. 218. [CrossRef]
31. Couture, T.D.; Becker-Birck, C. Energy policy design for low and middle income countries: From best practices to 'Next' practices. In *Renewable Energy for Unleashing Sustainable Development*; Springer: Cham, Switzerland, 2013; pp. 239–251. [CrossRef]
32. Yang, H.; Lu, L.; Zhou, W. A novel optimization sizing model for hybrid solar-wind power generation system. *Sol. Energy* **2007**, *81*, 76–84. [CrossRef]
33. Diaf, S.; Diaf, D.; Belhamel, M.; Haddadi, M.; Louche, A. A methodology for optimal sizing of autonomous hybrid PV/wind system. *Energy Policy* **2007**, *35*, 5708–5718. [CrossRef]
34. Bernal-Agustìn, J.L.; Dufo-Lòpez, R. Simulation and optimization of stand-alone hybrid renewable energy systems, *Renew. Sustain. Energy Rev.* **2009**, *13*, 2111–2118. [CrossRef]
35. Atashpaz-Gargari, E.; Lucas, C. Imperialist competitive algorithm: An algorithm for optimization inspired by imperialistic competition. In Proceedings of the 2007 IEEE Congress on Evolutionary Computation, Singapore, 25–28 September 2007; pp. 4661–4667. [CrossRef]
36. Alliance for Rural Electrification. Using Batteries to Ensure Clean, Reliable and Affordable Universal Electricity Access. 2013. Available online: https://www.ruralelec.org/publications/using-batteries-ensure-clean-reliable-and-affordable-universal-electricity-access (accessed on 31 March 2020).
37. Merz, K.D.; Crugnola, G.; Bonduelle, G.; Bruggeman, R.; Linck, F.; Linke, R.; Cilia, J.; Chris, H.; Marckx, E. Battery Energy Storage for Rural Electrification Systems. 2013. Available online: https://www.eurobat.org/images/news/position-papers/eurobat_rural_may_2013.pdf (accessed on 31 March 2020).
38. Akinyele, D.; Rayudu, R. Review of energy storage technologies for sustainable power networks. *Sustain. Energy Technol. Assessments* **2014**, *8*, 74–91. [CrossRef]
39. Bloomberg New Energy Finance. New Energy Outlook 2017. Available online: https://about.bnef.com/new-energy-outlook/ (accessed on 31 March 2020).
40. Boston Power. Datasheet—Swing 5300. Available online: http://www.boston-power.com.cn (accessed on 31 March 2020).
41. Fleer, J.; Zurmühlen, S.; Badeda, J.; Stenzel, P.; Hake, J.; Sauer, D.U. Model-based economic assessment of stationary battery systems providing primary control reserve. In Proceedings of the 10th International Renewable Energy Storage Conference—IRES, Düsseldorf, Germany, 15–17 March 2016. [CrossRef]
42. Brivio, C.; Musolino, V.; Alet, P.J.; Merlo, M.; Hutter, A.; Ballif, C. Analysis of lithium-ion cells performance, through novel test protocol for stationary applications. In Proceedings of the 2017 6th International Conference on Clean Electrical Power: Renewable Energy Resources Impact, ICCEP 2017, Puglia, Italy, 2–4 July 2017; pp. 410–415. [CrossRef]
43. He, H.; Xiong, R.; Fan, J. Evaluation of lithium-ion battery equivalent circuit models for state of charge estimation by an experimental approach. *Energies* **2011**, *4*, 582–598. [CrossRef]
44. Gomez, J.; Nelson, R.; Kalu, E.E.; Weatherspoon, M.H.; Zheng, J.P. Equivalent circuit model parameters of a high-power Li-ion battery: Thermal and state of charge effects. *J. Power Sources* **2011**, *196*, 4826–4831. [CrossRef]
45. Gao, Y.; Jiang, J.; Zhang, C.; Zhang, W.; Ma, Z.; Jiang, Y. Lithium-ion battery aging mechanisms and life model under different charging stresses. *J. Power Sources* **2017**, *356*, 103–114. [CrossRef]
46. Brivio, C. Battery Energy Storage Systems: Modelling, Applications and Design Criteria. Ph.D. Thesis, Politecnico di Milano, Milan, Italy, 2017.
47. Birkl, C.R.; Roberts, M.R.; McTurk, E.; Bruce, P.G.; Howey, D.A. Degradation diagnostics for lithium ion cells. *J. Power Sources* **2017**, *341*, 373–386. [CrossRef]

48. He, G.; Chen, Q.; Kang, C.; Pinson, P.; Xia, Q. Optimal Bidding Strategy of Battery Storage in Power Markets Considering Performance-Based Regulation and Battery Cycle Life. *IEEE Trans. Smart Grid* **2016**, *7*, 2359–2367. [CrossRef]
49. Zhuo, W.; Savkin, A.V. Profit Maximizing Control of a Microgrid with Renewable Generation and BESS Based on a Battery Cycle Life Model and Energy Price Forecasting. *Energies* **2019**, *12*, 2904. [CrossRef]
50. Xu, B.; Oudalov, A.; Ulbig, A.; Andersson, G.; Kirschen, D.S. Modeling of Lithium-Ion Battery Degradation for Cell Life Assessment. *IEEE Trans. Smart Grid* **2018**, *9*, 1131–1140. [CrossRef]
51. Dubarry, M.; Qin, N.; Brooker, P. Calendar aging of commercial Li-ion cells of different chemistries—A review. *Curr. Opin. Electrochem.* **2018**, *9*, 106–113. [CrossRef]
52. Dufo-López, R.; Lujano-Rojas, J.M.; Bernal-Agustín, J.L. Comparison of different lead-acid battery lifetime prediction models for use in simulation of stand-alone photovoltaic systems. *Appl. Energy* **2014**, *115*, 242–253. [CrossRef]
53. Pfenninger, S.; Staffell, I. Long-term patterns of European PV output using 30 years of validated hourly reanalysis and satellite data. *Energy* **2016**, *114*, 1251–1265. [CrossRef]